GEOG 321 - Reading Package Lectures 14

RADIATION ON SLOPES

The radiation received by a surface is usually the major determinant of its climate. This radiant input is composed of the components $K_{\downarrow} = S + D$ and $L_{\downarrow}$, of which only the direct-beam receipt (S) is dependent upon the angle at which it strikes the receiving surface.

Calculation of direct beam irradiance on slopes. In order to calculate the beam radiation $\hat{S}$ at a point on a slope it is necessary to add further geometric relations in addition to the ones introduced in Lecture 4 (See Reading Package Lectures 4-5, Equations 2.6 - 2.10).

In addition to solar zenith Z we need to introduce also an equation for the *solar azimuth* Ω. Ω is the angle between the projections onto the horizontal plane of the site of both the Sun and the direction of true north. The azimuth angle is measured clockwise from north (0 - 360°) If $t < 12$ (i.e. morning):

$$\cos\Omega = \frac{\sin\delta\cos\phi - \cos\delta\sin\phi\cos h}{\sin Z} \qquad (9.1)$$

If $t > 12$ (i.e. afternoon):

$$\cos\Omega = 360° - \frac{\sin\delta\cos\phi - \cos\delta\sin\phi\,\mathrm{cosh}}{\sin Z} \qquad (9.2)$$

The diagram in Figure 1 depicts a non-horizontal surface with an approximately SW aspect. The geometry of the solar beam (yellow) is defined using the zenith angle Z and the solar azimuth angle Ω, both of which are illustrated in Figure 1 for a slope. In order to aid definition of the angles an imaginary horizontal plane is constructed through the point of interest (i.e. the dot at mid-slope). The slope is inclined at the angle $\hat{\beta}$ to the horizontal and has the azimuth $\hat{\Omega}$. The latter is the angular measurement (degrees) between the projection of true north onto the horizontal plane and the line formed by the intersection of the horizontal plane with that formed by the vertical plane extending downwards from the normal to the slope.

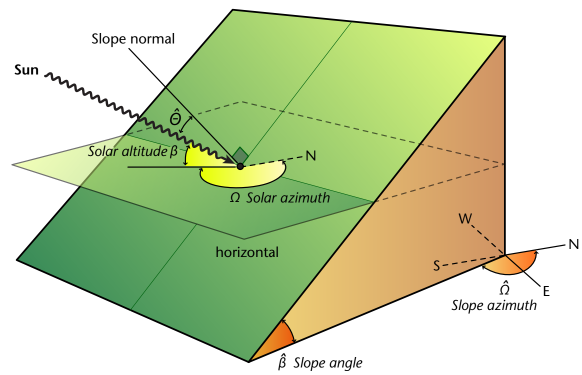

Figure 1: Geometry for solar beam irradiance of a sloping plane (see text for details).

The best way to relate the slope and solar geometries is to use the angle of incidence ($\hat{\Theta}$) between the normal to the slope and the solar beam, where:

$$\hat{\Theta} = \cos\hat{\beta}\cos Z + \sin\hat{\beta}\sin Z\cos(\Omega - \hat{\Omega}) \qquad (9.3)$$

Then the direct-beam solar radiation on a slope ($\hat{S}$) is given in terms of the beam radiation at normal incidence (S_i) by:

$$\hat{S} = S_i\cos\hat{\Theta} \qquad (9.4)$$

and based on the cosine law of illumination in terms of the beam radiation received on the horizontal (S) by:

$$\hat{S} = \frac{S\cos\hat{\Theta}}{\cos Z} \qquad (9.5)$$

The daily and annual course of $\hat{S}$ on slopes of various angles and azimuths (aspects) at latitude 49° can be calculated using the applet on the course webpage[1]

Effects of slope geometry. At a given time and location S_i is unlikely to vary very much spatially (depending upon atmospheric conditions) and hence variations in the slope and azimuth angles presented by topography determine the radiant loading differences across a landscape. Clearly the slope that most directly faces the Sun (i.e. where $\hat{\Theta}$ approaches zero, and therefore

[1] http://www.geog.ubc.ca/courses/geob300/applets/slope/

$\cos\hat{\Theta}$ approaches unity) will receive the most radiation; whereas if the Sun is almost grazing the surface (i.e. $\hat{\Theta}$ approaches 90°, and cos $\hat{\Theta}$ approaches zero) minimal radiation is received. Because of the cosine form it can be seen that the direct beam solar input is almost uniformly high for angles of $\hat{\Theta}$ less than 30°, but at great angles receipt drops at an increasing rate. Figure 2 shows the daily input of direct-beam radiation to various slope angles and aspects at latitude 40°N at the times of the solstices (when the Sun is overhead at the Tropics of Cancer and Capricorn); and equinoxes (when the Sun is overhead at the Equator). In the northern hemisphere, south-facing and horizontal surfaces show symmetrical energy receipt centred on midday.

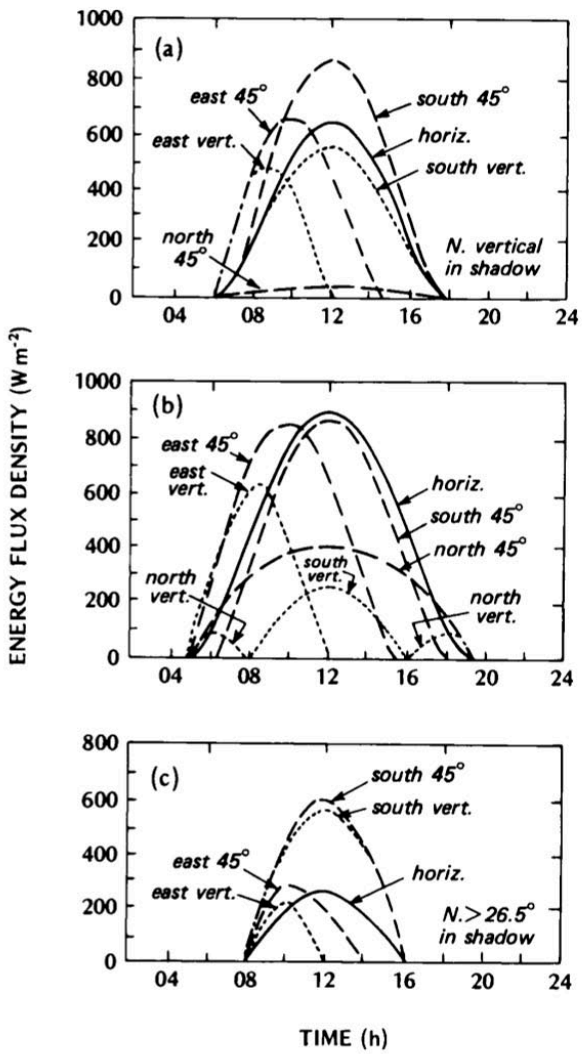

Figure 2: The diurnal variation of direct-beam solar radiation upon surfaces with different angles of slope and aspect at latitude 40°N for (a) the equinoxes (21 March, 21 September), (b) summer solstice (22 June), and (c) winter solstice (22 December) (after Gates, 1965).

At the equinoxes the maximum direct-beam input will be upon a south- facing slope of 40° at midday (i.e. $\hat{\Theta}$ = zero because the Sun is overhead and $\hat{S} = S_i$). The closest slope to this in Figure 2a is south 45° ($\hat{\Theta}$ = 5°), next is horizontal ($\hat{\Theta}$ = 40°) and then south vertical ($\hat{\Theta}$ = 50°). East-facing slopes receive the early morning solar beam more effectively than the south- facing slopes. Hence the curves for east-facing slopes rise more sharply after sunrise, with the east 45° slope receiving more than the east vertical. However as the Suns azimuth changes through the day, east-facing slopes soon achieve their 'local solar noon', and the incident radiation decreases rapidly towards their 'local sunset' (12 h for east vertical, and 15 h for east 45°). Although not shown in Figure 2a the situation for west-facing slopes would be symmetrical with that of the east-facing slopes, showing higher receipts in the late afternoon than the south-facing slopes. At the times of the equinoxes vertical north-facing slopes receive no direct-beam shortwave radiation input, their radiant receipt being limited to diffuse shortwave and longwave radiation from the atmosphere. The input to a north 45° slope is very slight at all times.

At the summer solstice (Figure 2b) the horizontal, east- and north-facing slopes experience sunrise before the south- and west-facing slopes (west is not shown but is symmetrical with east). East-facing slopes are illuminated as for the equinoxes but with an earlier sunrise, and a larger maximum input. Horizontal surfaces receive direct-beam radiation throughout the day, and of the slopes shown they obtain the maximum intensity at the midday peak (for a horizontal surface $\hat{\Theta}$ = 16.5°, for south 45° $\hat{\Theta}$ = 28.5, and for south $\hat{\Theta}$ = 73.5° vertical). The vertical north- and south-facing slopes show mutually exclusive illumination, the north being in receipt early and late in the day (experiencing two sunrises and sunsets per day), and the south only in receipt between 08 h and 16 h.

By the winter solstice (Figure 2c), north-facing slopes of greater than 26.5° receive no direct-beam at all, whereas south-facing slopes are most favourably placed. The length of day is considerably shorter, which combined with the generally lower intensities give relatively small daily radiation incomes. In general the effect of moving from high to low latitude is to increase the illumination of the north-facing slopes at the expense of the south- facing slopes. Also, since the Sun is never more than 47° from the zenith at midday in the tropics, the effect of topographic slope changes is reduced compared to high latitudes where small slope or aspect changes may be of considerable practical importance.

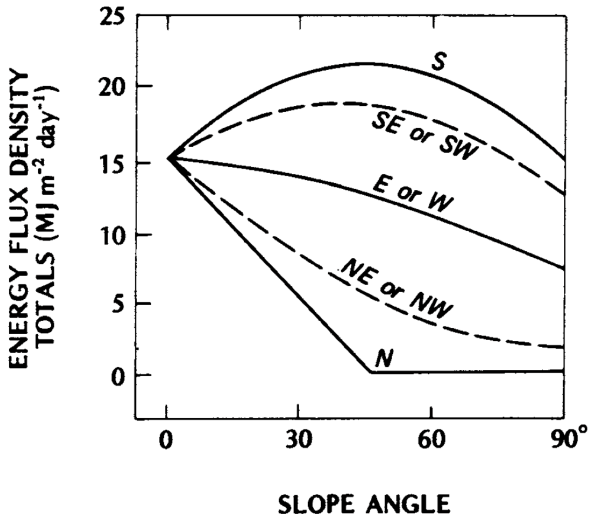

Figure 3: Total daily direct-beam solar radiation ($\hat{S}$) incident upon slopes of differing angle and aspect at latitude 45N at the times of the equinoxes (diagram constructed by Monteith, 1973, using data from Garnier and Ohmura, 1968).

Figure 3 gives the direct-beam shortwave radiation totals at the time of the equinoxes at latitude 45°N (approximately equivalent to Figure 2a). It shows marked differences in the receipt of direct-beam radiation on slopes of different aspect. Note that the maximum load would be on a south 45° slope ($\hat{\Theta}$ = 0°), whereas no direct-beam would reach north-facing slopes of greater than 45° angle. In a Geographic Information System or using programming, direct-beam radiation can be modelled by determining the slope angle and azimuth for each grid position, and then computing the radiant input. Spatial energy distributions of this type form an excellent base for the understanding of micro-climatic variations in regions of complex topography. Most modern GIS systems are able to calculate $\hat{S}$ and also account for shading by nearby mountains.

Diffuse irradiance. Although only an approximation, we may assume that diffuse shortwave input D from cloudless and cloudy skies is equal for all positions of the sky hemisphere, and therefore does not contribute to spatial variability of solar receipt at the surface. But the receipt of direct-beam under partial cloud cover clearly gives marked differences between areas in direct illumination and those in shadow from cloud. If the cloud is in motion, rather than occupying preferred positions, then over a sufficient period of time such differences will average out spatially. On the other hand, cloud may be directly related to surface features such as sea breeze or anabatic cloud. This leads to different solar loading across the landscape which may re-inforce or dampen the cause of cloud development.

ENERGY BALANCE ON SLOPES

Topographically-induced radiation variations lead to energy balance differences across the landscape. An example is given in Table 1 that shows the south-facing slope receives almost three times more net radiation than the north-facing slope. Some of the increase can be attributed to the lower albedo of the south-facing slope, but the primary effect is probably due to its more favourable aspect. The slope surfaces were bare debris, and the local climate was semi-arid, which accounts for the energy balance partitioning in favour of sensible heat (Q_H), and the high values of Bowens ratio ($\beta = Q_H/Q_E$) values. However, the south-facing slope pumps more than three times as much sensible heat into its lower atmosphere; such strong differential heating is likely to produce local slope winds (See Lecture 30). The lower β value for the north-facing slope may also indicate a greater availability of moisture for evaporation.

It is evident therefore that orientation of a surface with respect to the solar beam is a very powerful variable in determining its energy income. It also follows that the naturally uneven configuration of the landscape produces a wide spectrum of microclimates, and these have implications for other aspects of the physical environment. Plant and animal habitats are impacted, leading to distinctly different assemblages of flora and fauna on slopes of different angle and aspect. Similarly these differences are often reflected in the type of land-use especially in agriculture and forestry.

Hydrologic activity is also likely to vary as a result of different rates of evaporation, lengths of snow cover retention, and probabilities of avalanching on different slopes. Geomorphic processes such as frost-shattering, mud slumping, soil creep, and rock exfoliation are directly or indirectly sensitive to such thermal and/or moisture variations.

Site	Energy balance				Dimensionless quantities		
	Q^*	Q_H	Q_E	Q_G	α	β	Q_E/Q^*
Horizontal	14·4	9·4	2·1	2·1	0·14	4·5	0·15
North-facing (33°)	6·0	3·5	1·7	0·7	0·20	2·0	0·28
South-facing (31°)	17·6	12·6	3·1	1·9	0·15	4·1	0·18

Table 1: Effects of topography on the surface energy balance of bare ground in the Turkestan Mountains (41°N). Data are daily energy totals (MJ m^{-2} day^{-1}) based on monthly average for September (from Aisenshtat, 1966).